Improvement of maximum power point tracking in photovoltaic arrays in different environments using hybrid algorithms*

ZHANG Jiuchao, REN Guangjun, XUE Yuming, XIA Dan, WANG Jiangchao, and HU Zhaoshuo**
Institute of New Energy Intelligence Equipment, School of Integrated Circuit Science and Engineering, Tianjin University of Technology, Tianjin 300384, China

(Received 10 October 2022; Revised 18 November 2023)

When the photovoltaic (PV) system is generating PV power, the partial shading (PS) condition will cause multiple peaks in the power-voltage curve, and changes in light intensity and ambient temperature will cause the curve to shift. Traditional maximum power point tracking (MPPT) methods, such as the incremental conductance (INC) method, have the problem of being trapped in the local optimal solution. Biomimetic optimization algorithms, such as particle swarm optimization (PSO), have problems with oscillation and low tracking efficiency near the global maximum power point (GMPP). As a result, a hybrid algorithm CS-INC based on the cuckoo search (CS) algorithm and the perturb and observe (P&O) approach is proposed in this study. The light intensity remains constant, the light intensity changes in steps, and the partial shade scenario are simulated. Simulation results show that the MPPT improves accuracy, speed, and stability.
Document code: A **Article ID:** 1673-1905(2024)01-0028-7
DOI https://doi.org/10.1007/s11801-024-2171-0

Electric energy consumption increases daily as the world population grows, business develops, and science and technology advance. Photovoltaic (PV) power generation has become widely commercialized worldwide because of its greenness, cleanliness, and extensive development prospects[1]. The government has expanded clean energy support and subsidies, and promoted PV power plant building[2].

In general, a key task of PV systems is to capture the most solar energy quickly, a process called maximum power point tracking (MPPT)[3]. However, in some circumstances, the output efficiency of PV systems cannot be maintained due to environmental conditions. The *P-V* curves, representing the output characteristic curves of PV cells, are nonlinear and primarily affected by light intensity and temperature. Generally, there is a specific point on the output characteristic curve. The PV system operates at this point for maximum power[4]. The *P-V* characteristic curve has a peak value when the PV array's light intensity is uniform. The characteristic curve fluctuates as light intensity and temperature change. This curve features many peaks when the PV array is in partial shade, with the greatest peak allowing the PV system to output the maximum power[5]. As a result, to achieve maximum power, the PV system requires a tracking controller with the largest peak[6]. Limit the design of a PV system MPPT scheme, including implementation complexity, energy consumption, and cost[7].

Look-up table[8], fractional short-circuit current (FSCC)[9], and fractional open-circuit voltage (FOCV)[10] are the essential components of the original MPPT technology. The advantage of these techniques is that they rely on a priori data and do not require continuous tracking of PV cell current and voltage. However, as light intensity and temperature fluctuate, this approach does not accurately track MPP. An intermittent FOCV MPPT algorithm[11], an adaptive-fractional-open-circuit-voltage (AFOCV) MPPT circuit[12], has been proposed to reduce energy loss under mismatch and environmental changes.

MPPT approaches in the second category include hill-climbing (HC)[13], incremental conductance (INC)[14], and perturb and observe (P&O)[15]. These technologies necessitate collecting real-time data on ambient light intensity and temperature. The MPP can be tracked as the ambient light intensity and temperature vary. However, in the case of small reference voltage steps, when the light intensity changes suddenly, the dynamic performance is poor. In the case of partial shading (PS), such strategies are stuck in local optimal solutions. If the step size of the reference voltage is increased, it will cause a large steady-state oscillation and increase the energy loss. Aiming at the shortcomings of the traditional

* This work has been supported by the Science and Technology Innovation Development Program (No.70304901).
** E-mail: orwellx@tjut.edu.cn

conductance increment method, a new modified variable-step INC algorithm[16] is proposed, which improves the efficiency of MPPT.

In order to accurately track the MPP in the case of partial shadow, some bionic optimization methods are applied to MPPT. In Ref.[17], the particle swarm optimization (PSO) MPPT technology is used in conjunction with the boost converter to accurately measure global maximum power point (GMPP). In Ref.[18], the bat algorithm is utilized in the MPPT and improved on this basis. In Ref.[19], the coyote optimization algorithm is used to solve the reconstruction problem of partially shading PV arrays. Cuckoo search (CS) is a method that is gaining much traction. In Ref.[20], the improved CS algorithm is applied to the MPPT. However, these algorithms also suffer from some drawbacks. For example, the oscillation near the global maximum value and the complexity of the algorithm cause the problem of low tracking efficiency of the GMPP.

This study offers a hybrid algorithm (CS-P&O) that combines the CS algorithm with the P&O to overcome the shortcoming of the P&O method falling into the local optimal solution and the steady-state oscillation of the CS algorithm. The CS strategy can jump out of the local optimal solution while the P&O method suppresses steady-state oscillation and quickly finds the global optimal solution. The P&O approach is used with the CS algorithm. MPPT is possible with constant light intensity, varied light intensity, and partial shadows. The proposed hybrid algorithm can handle anomalous conditions to the greatest extent possible while increasing efficiency and convergence speed and reducing steady-state oscillations.

Modeling PV cells is the initial step in designing a PV power generation system. The performance of PV power generation systems is closely tied to the model of PV cells. A proper solar cell model can reflect the PV power generation system's actual performance characteristics[19]. Fig.1 depicts a commonly used PV cell equivalent circuit. According to Fig.1, the output characteristic expression of the PV cell can be obtained as follows

$$I_{\mathrm{L}} = I_{\mathrm{ph}} - I_{\mathrm{D}} - \frac{U_{\mathrm{D}}}{R_{\mathrm{sh}}}, \tag{1}$$

$$I_{\mathrm{L}} = I_{\mathrm{ph}} - I_{\mathrm{O}} \left\{ \exp\left[\frac{q\left(U_{\mathrm{OC}} + I_{\mathrm{L}} R_{\mathrm{s}}\right)}{AkT} \right] - 1 \right\} - \frac{U_{\mathrm{D}}}{R_{\mathrm{sh}}}, \tag{2}$$

where

$$I_{\mathrm{ph}} = \left[I_{\mathrm{SC}} + K_{\mathrm{t}} \left(T - T_{\mathrm{r}} \right) \right] \frac{G}{1\,000}, \tag{3}$$

$$I_{\mathrm{O}} = I_{\mathrm{or}} \left[\frac{T}{T_{\mathrm{r}}} \right] \exp\left[\frac{qE_{\mathrm{g}}}{Bk} \left(\frac{1}{T_{\mathrm{r}}} - \frac{1}{T} \right) \right]. \tag{4}$$

The symbols used in the above formulas are explained in Tab.1. Eqs.(1)—(4) show that the output characteristics of PV cells are affected by light intensity and temperature.

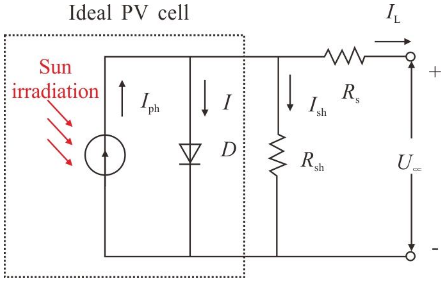

Fig.1 Equivalent circuit diagram of PV cell

Tab.1 Interpretation of symbols used in formulas

Symbol	Interpretation	Symbol	Interpretation
I_{L}	Output current	k	Boltzmann constant
U_{OC}	Open circuit voltage	I_{SC}	Short circuit current
I_{ph}	Photocurrent	T	Temperature
I_{D}	Diode forward conduction current	T_{r}	The rated operating temperature
I_{O}	Reverse saturation current	E_{g}	Band gap
A, B	Ideality factor	G	Light intensity

A PV array can be formed by connecting individual PV cells in series and parallel. PV power plants often use this method to obtain more power. The following equation describes the relationship between PV array output current and voltage[21]

$$I_{\mathrm{L}} = N_{\mathrm{s}} I_{\mathrm{ph}} - N_{\mathrm{p}} I_{\mathrm{or}} \left(\exp\left[\frac{q}{AkT_{\mathrm{c}}} \left(\frac{U_{\mathrm{OC}}}{N_{\mathrm{s}}} + \frac{R_{\mathrm{s}} I_{\mathrm{L}}}{N_{\mathrm{p}}} \right) \right] - 1 \right), \tag{5}$$

where N_{s} and N_{p} represent the numbers of PV cells in series and parallel, respectively.

When a PV system is used, it is generally blocked by trees, clouds, or buildings. The light intensity of the PV cells in the solar array will be unequal due to the shading, which is known as PS[22].

A bypass diode is commonly connected in reverse parallel to the solar cell to prevent this effect from damaging the PV system. In addition, an anti-backflow diode needs to be connected in series at the end of each PV array string to prevent the reverse current between different PV array strings. Fig.2 shows the PV system model under uniform light intensity and partial shade. In general, diodes protect the PV system from the above hazards. However, it will inevitably lead to a change in the output characteristic curve of the PV array. In Fig.3, the power characteristic curve when the light intensity of the PV array is uniform has GMPP. The *P*-*V* characteristic curve has many local maximum power points (LMPPs) and one GMPP when the PV system is partially shaded.

The P&O method necessitates using current and voltage data for MPP tracking. Its working principle is as follows. In one cycle, the output voltage of the PV cell is perturbed according to a certain perturbation step. The direction of the next disturbance is determined by judging the power value after the disturbance and the power value before the disturbance.

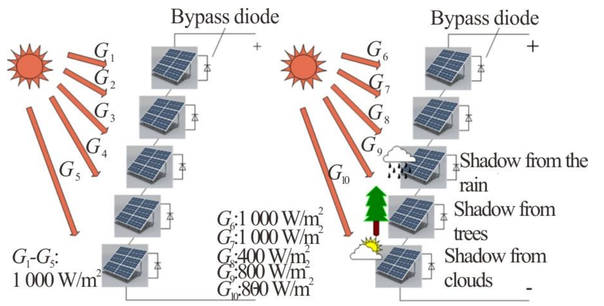

Fig.2 PV system model with uniform light intensity and partial shade

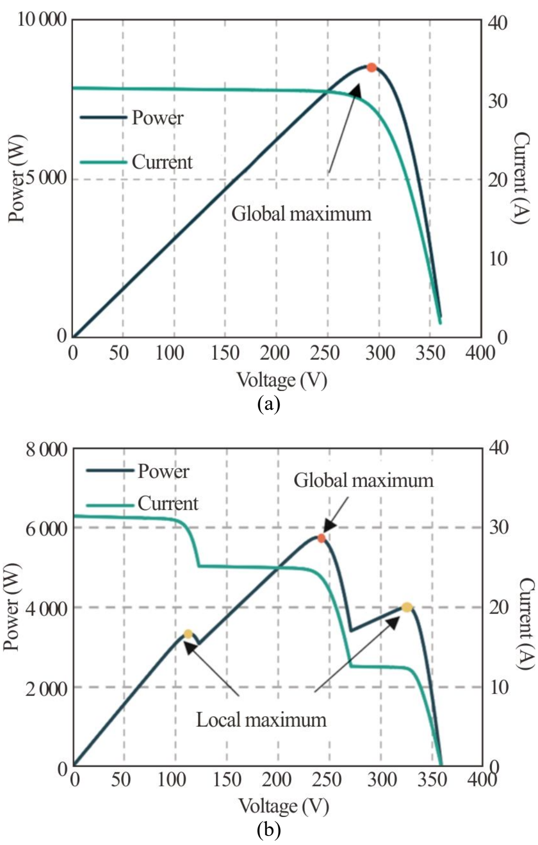

Fig.3 Output characteristic curves under (a) uniform light intensity and (b) partially shaded conditions

Fig.4 is a schematic diagram of the working principle of P&O, and the specific control steps are as follows.

(1) Apply disturbance $+\Delta U$. If $\Delta P>0$, it is reflected in the movement of the working point from point A to point B in the figure. Since the MPP C is located to the left of point B, the perturbation $+\Delta U$ continues to be applied until the power increases to P_{m}.

(2) Apply disturbance $+\Delta U$. If $\Delta P<0$, it is reflected in the movement of the working point from point C to point D in the figure. Since the MPP C is located to the left of point D, the perturbation $-\Delta U$ continues to be applied until the power increases to P_{m}.

(3) Apply perturbation $-\Delta U$. If $\Delta P>0$, it means that the operating point is on the right side of the MPP C and moves to point C. At this time, continue to apply perturbation $-\Delta U$ to reach the point P_{m}.

(4) Apply perturbation $-\Delta U$. If $\Delta P<0$, it means that the operating point is on the left side of the MPP C and moves away from point C. At this time, continue to apply disturbance $+\Delta U$ to reach the point P_{m}.

Follow this step until the output power remains basically unchanged after the disturbance is applied again, which indicates that the MPP has been tracked.

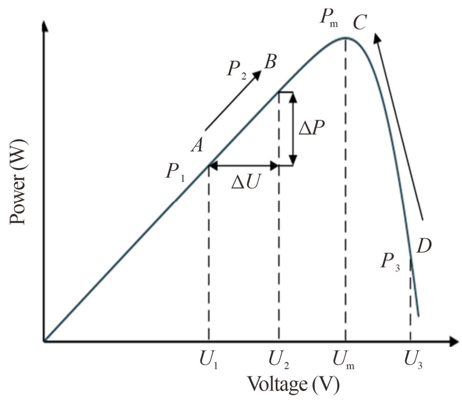

Fig.4 Schematic diagram of the working principle of P&O

CS is a biomimetic optimization technique based on cuckoos' parasitic reproduction mechanism. Some cuckoo species lay their eggs in the nests of other birds (host birds) in nature, a practice known as nest parasite brooding[23]. Finding an appropriate host nest is the first step in nest-hosting brooding behavior. The procedure of locating a host bird's nest is similar to locating food for an animal. Mathematical models can generally depict animals' direction and trajectory when searching for food. Lévy flight[24] is a model based on the flies' feeding paths invented. Fruit fly flight trajectories are unpredictable, with no discernible pattern and even abrupt 90° turns in some cases. Lévy flight covers a more extensive region with fewer steps and distance, making it ideal for exploring new territory. The cuckoo's hunt for the nest is known as Lévy flight in the CS algorithm. In a two-dimensional plane, Fig.5 displays a Lévy flight.

After deciding on it, the cuckoo will place its eggs in the host nest. When the host bird discovers a cuckoo egg, most host birds destroy it, and some even abandon their nest[25].

Several idealized rules for cuckoo parasitism were proposed[26]. (1) Cuckoos only lay one egg at a time and parasitize it in randomly selected nests. (2) The best nests will be retained from a randomly selected set of nests for the future generation. (3) The numbers of eggs laid and available nests are fixed. P_{a} ($0<P_{\mathrm{a}}<1$) is the likelihood that the nest owner will find the exotic bird eggs. If a cuckoo's egg is discovered, the host bird has the option of destroying or abandoning its nest. A new nest is created in either cause. While the cuckoo is looking for a new nest, the Lévy flight is performed as follows

$$x_i^{(t+1)} = x_i^t + \alpha \oplus \text{Levy}(\lambda), \tag{6}$$

where

$$\alpha = \alpha_0 \left(\chi_j^{(t)} - \chi_i^{(t)} \right), \tag{7}$$

$$\text{Levy}(\lambda) \approx u = l^{-\lambda}, (1 < \lambda < 3), \tag{8}$$

where x_i^t is the sample position, i is the number of samples, t is the number of iterations, λ is the step size, and α_0 is the initial step change.

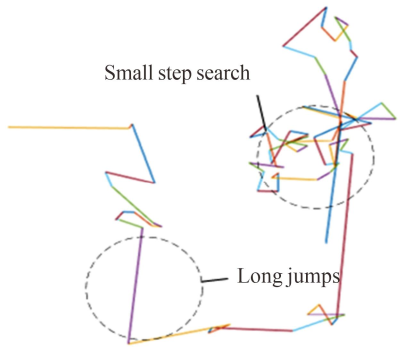

Fig.5 Example of Lévy flying in the two-dimensional plane

In the CS-INC algorithm, set the number of bird's nests to n, initialize the location of the bird's nest P_0, and determine the optimal bird's nest $x_b^{(0)}$. In order to apply the CS algorithm to the MPPT system, appropriate variables must be selected for the search. The nest is defined as the voltage of a PV cell, i.e., U_i. Define the total number of samples as n, the step size as α, and P_i as the value of the power corresponding to the voltage U_i in the P-V curve. The position of the optimal bird's nest $x_b^{(0)}$ corresponds to the voltage value at the MPP in the MPPT system. In an MPPT system, a new voltage sample is created using the following formula

$$U_i^{(t+1)} = U_i^t + \alpha \oplus \text{Levy}(\lambda), \tag{9}$$

where $\alpha = \alpha_0(v_{\text{best}} - v_i)$. The simplified Lévy flight strategy is as follows

$$s = \alpha_0 \left(v_{\text{best}} - v_i \right) \oplus \text{Levy}(\lambda) \approx \kappa \times \left(\frac{u}{(|v|)^{\frac{1}{\beta}}} \right) \left(v_{\text{best}} - v_i \right), \tag{10}$$

where β=1.5, and k is the Lévy flight factor in this design.

To search the complete P-V curve, the initial samples must be dispersed across the entire voltage range. The key is the number of samples n. The larger the n, the more efficient the search (i.e., the more likely it is to find the correct value), but the longer the convergence time. Based on many simulations, n=3 appears to be a good compromise in the MPPT problem and is thus employed throughout the work.

Set the values of all constants and variables, including voltage, current, power, the number of samples, and the value of β. The power is calculated using the current-voltage and current values. By comparing the power values, the maximum power produced by the voltage is picked as the new best sample. All save this best sample was destroyed at random with probability P_a, a method that simulates the behavior of a host bird detecting and destroying cuckoo eggs. Then, to replace the corrupted samples, new random samples are generated.

Before each iteration begins, a check is made to see if the samples have attained convergence. The samples will merge to the same value if they have converged to MPP. If the samples do not converge, the P_i^t array measures and stores all power values for the related samples. The sample with the highest power is chosen as the best sample once the array has been evaluated. After that, all other samples are compelled to move closer to this optimal value. Set a number of iterations. If the number of iterations is less than a certain value, continue to execute the CS and start the P&O method when the number of iterations is not less than this value. After that, the MPP was searched by the incremental P&O method. The overall flow chart of CS-P&O MPPT is shown in Fig.6.

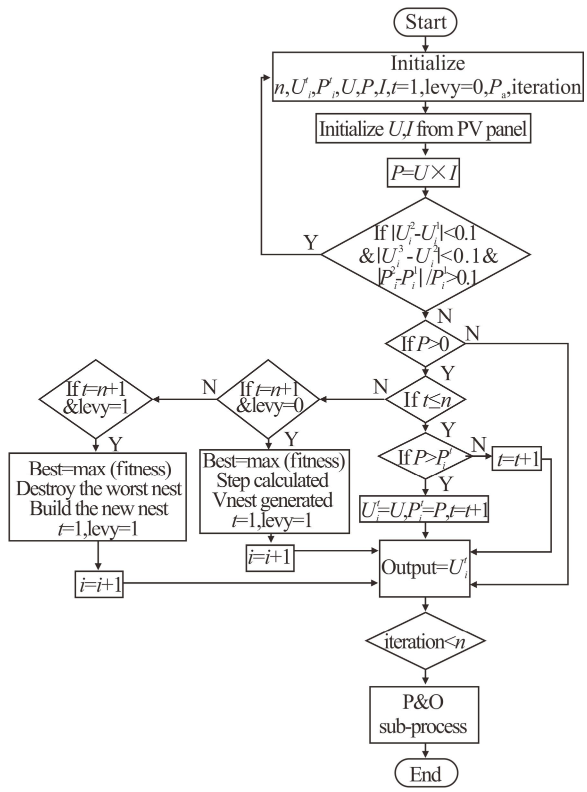

Fig.6 Overall flow chart of CS and P&O MPPT

The circuit diagram for the MPPT simulation test is shown in Fig.7. Five PV sub-arrays are employed in series in this experiment, with each PV sub-array consisting of eight PV cells in four series and two parallels. A bypass diode is connected in reverse parallel to each PV sub-array to form a PV array. Each PV cell has the same set of parameters listed in Tab.2.

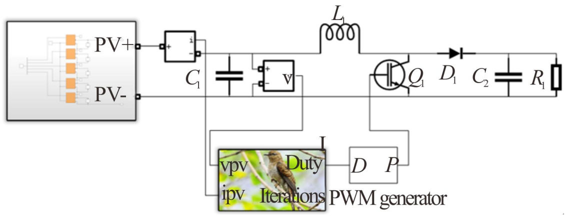

Fig.7 Circuit diagram of MPPT simulation test

Tab.2 Description of the parameters of the PV calls used in this paper

Parameter	Label	Value
Maximum power	P_{MPP}	213.15 W
Open circuit voltage	V_{OC}	36.3 V
Short-circuit current	I_{SC}	7.84 A
The voltage at MPP	V_{mp}	29 V
Current at the P_{MPP}	I_{mp}	3.35 A
Temperature coefficient of V_{OC}	K_V	−0.361%/°C
Temperature coefficient of I_{SC}	K_I	0.102%/°C

The following is the circuit specifications for the MPPT simulation test: switching frequency is f=20 kHz, inductance is L=8.587 8 mH, capacitance is C=20.255 μF, C_{pv}=500 μF, and resistance is R=20 Ω.

The temperature is 25 °C, and the light intensity of all PV cells in the solar array is 1 000 W/m^2. At this time, the MPP of the PV array is 8 518 W. The simulation results are shown in Fig.8. It can be observed from the figure that CS-P&O tracks MPP faster than CS. The reason for this phenomenon is that after CS-P&O is iterated, CS switches to P&O with a faster tracking speed. The tracking of MPP by PSO is the slowest, taking 0.884 s. After tracking to the MPP, the operating point of the CS-P&O remains firmly at the MPP, i.e., the oscillation is almost zero. This is due to the small step size set by the P&O. The PSO and CS oscillated after tracking the MPP. The results of this test show that when the light intensity and temperature remain unchanged, the tracking speed and stability of CS-P&O are improved compared with CS and PSO.

A cloud passing over to hide the sun on a clear day might create a step-change in light intensity. The temperature of the test was always kept at 25 °C. Tab.3 shows the MPP for each period.

This test evaluates the CS-P&O and several other algorithms' response speed and MPP's re-tracking when the light intensity suddenly changes. Fig.9 shows CS-P&O and several other algorithms' simulation results. As the diagram shows, both CS-P&O and several other algorithms can respond when the light intensity suddenly lowers and increases. The reason for the slower INC tracking is the small step size used to reduce steady-state oscillations. Several other biomimetic optimization algorithms are faster, while PSO shows larger steady-state oscillations. Due to the more significant step size of the Lévy flight, the CS-P&O responds faster and can quickly track the MPP.

Tab.3 Simulation conditions for stepwise changes in light intensity

Time (s)	G (W/m^2)	P_{MPP} (W)
0≤t<1.5	1 000	8 518
1.5≤t<2.5	700	4 711
2.5≤t<4	1 000	8 518

When trees, clouds, or buildings block a portion of the solar array, the PV array's local light intensity diminishes. The P-V curve will have numerous peaks due to the bypass diode's action, i.e., several local peaks and one global peak. MPP tracking becomes more difficult in this circumstance.

The illumination intensities of the five PV sub-arrays were set to 1 000 W/m^2, 1 000 W/m^2, 400 W/m^2, 800 W/m^2, and 800 W/m^2 to simulate PS. At this time, the P-V curve of the PV array produces multiple peaks. The power of each peak is 3 334.07 W, 5 761.3 W, and 4 010 W, respectively.

The simulation results of CS-P&O and several other algorithms in the partially shaded case are shown in Fig.10. It can be observed from the figure that several bionic optimization algorithms can track GMPP. The maximum power value tracked by CS-P&O is 5 759.73 W, which is close to the global peak power in the c curve. This is due to the randomness of CS-P&O and the use of the Lévy flight strategy, so it jumps out of the local peak and tracks the GMPP. The CS-P&O is superior to CS and PSO in the tracking time of GMPP. This is because CS-P&O switches to P&O with a faster tracking speed after jumping out of LMPP. The maximum power value tracked by INC is 3 172.13 W, which is close to the peak value of the first local peak in the P-V curve. Therefore, INC gets stuck in local peaks.

In terms of MPPT speed, the maximum power tracked by various algorithms under different conditions is shown in the figure. When the light intensity is constant, the tracking speed of CS-P&O is 0.067 s, which is faster than 0.884 s of PSO and 0.167 s of CS. In the partially shaded case, the CS-P&O MPPT time is 0.068 s, which is also faster than PSO's 0.884 s and CS's 0.167 s.

In terms of the accuracy of MPPT, when the light intensity is constant and the light intensity changes stepwise, the PV array P-V curve has only one peak. All of these algorithms can accurately track the MPP, and the tracked MPP values are similar. Under the partial shade, CS tracks 3 172 W as it gets stuck in a local peak. The power tracked by CS-INC is 5 760 W. CS-INC is more accurate than INC in MPPT.

In terms of MPP steady-state oscillation, after CS-P&O tracks the MPP, the steady-state oscillation is almost zero, and the P-V curve is almost kept in a straight line. After the CS tracks the MPP, the power curve will oscillate. After the PSO tracks the MPP, the power curve will oscillate greatly. Sustained oscillations cause considerable power losses in some large PV power plants.

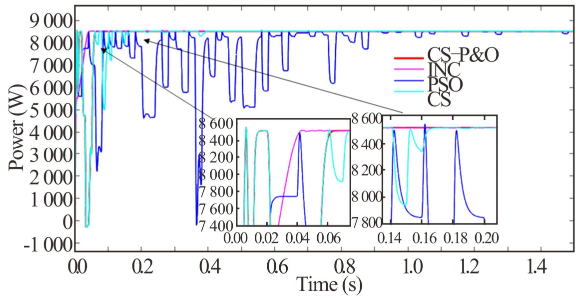

Fig.8 Simulation results with constant light intensity

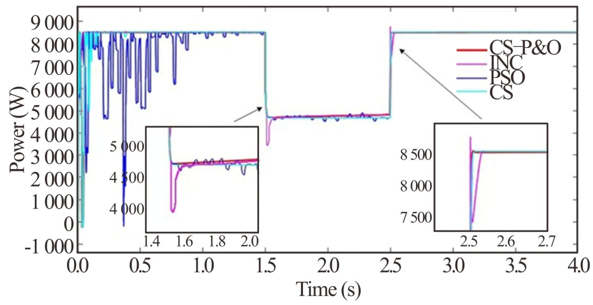

Fig.9 Simulation results for a step change in light intensity

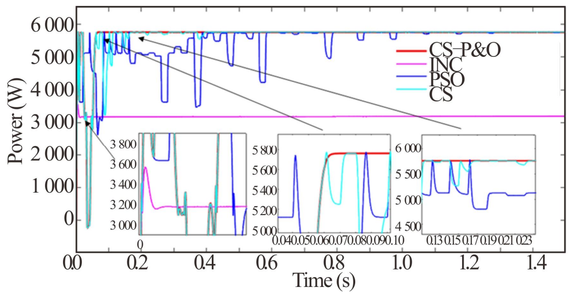

Fig.10 Simulation results for PS conditions

The CS algorithm and the P&O method are combined in this research to propose a hybrid MPPT method. Three different conditions were used to conduct comparative tests of different algorithms. The results show that this hybrid algorithm has a significant improvement in MPPT speed and steady-state oscillation. Compared to INC, the tracked power is 81.6% higher in partial shade. Under the condition of constant light intensity and partial shadow, the tracking speed of MPP is 13 times and 8.6 times that of PSO, and 2.5 times and 2.49 times that of CS, respectively. The algorithm's structure is also more straightforward to implement. It can be implemented with a low-performance microcontroller in practical applications. The solar array model and test environment employed in this experiment are more realistic in terms of PV array and test environment factors. The parameters of the components (capacitors, inductors) in the test circuit are also selected to suit the parameters of the solar cell array. The proposed hybrid method will next be implemented and verified in hardware.

Ethics declarations

Conflicts of interest

The authors declare no conflict of interest.

References

[1] BHUKYA L, NANDIRAJU S. A novel photovoltaic maximum power point tracking technique based on grasshopper optimized fuzzy logic approach[J]. International journal of hydrogen energy, 2020, 45(16): 9416-9427.

[2] CHEN S, LIU X, NIELSEN C, et al. Improved air quality in China can enhance solar-power performance and accelerate carbon-neutrality targets[J]. One earth, 2022, 5(5): 550-562.

[3] MOTAHHIR S, El HAMMOUMI A, EI GHZIZAL A. The most used MPPT algorithms: review and the suitable low-cost embedded board for each algorithm[J]. Journal of cleaner production, 2020, 246: 118983.

[4] HUYNH D C, DUNNIGAN M W. Development and comparison of an improved incremental conductance algorithm for tracking the MPP of a solar PV panel[J]. IEEE transactions on sustainable energy, 2016, 7(4): 1421-1429.

[5] FAN L S. Application in photovoltaic MPPT based on improved hysteresis loop comparison method[J]. Journal of physics, 2021, 2113: 1742-6588.

[6] MAO M, CUI L, ZHANG Q, et al. Classification and summarization of solar photovoltaic MPPT techniques: a review based on traditional and intelligent control strategies[J]. Energy reports, 2020, 6: 1312-1327.

[7] BIRANE M, LARBES C, CHEKNANE A. Comparative study and performance evaluation of central and distributed topologies of photovoltaic system[J]. International journal of hydrogen energy, 2017, 42(13): 8703-8711.

[8] DONG L K G. Optimal design of photovoltaic MPPT disturbance step length in a rapidly changing environment[J]. Journal of physics, 2021, 1: 1742-6596.

[9] VITORINO M A, HARTMANN L V, LIMA M N. An intelligent control strategy of fractional short circuit current maximum power point tracking technique for photovoltaic applications[J]. Journal of renewable and sustainable energy, 2015, 7(1): 15.

[10] AHMED B. A hybrid MPPT technique for solar photovoltaic system under partial shading[J]. Engineering proceedings, 2021, 12(1): 28.

[11] IM Y C, KWAK S S, PARK J, et al. Intermittent FOCV using an I-V curve tracer for minimizing energy loss[J]. Sciences-Basel, 2021, 11(19): 9006.

[12] HUANG P C, KUO T H. A 100-pA adaptive-FOCV MPPT circuit with >99.6% tracking efficiency for

indoor light energy harvesting[C]//15th IEEE Asian Solid-State Circuits Conference (A-SSCC), November 4-6, 2019, Macau, China. New York: IEEE, 2019: 185-188.

[13] JATELY V, AZZOPARDI B, JOSHI J, et al. Experimental analysis of hill-climbing MPPT algorithms under low irradiance levels[J]. Renewable and sustainable energy reviews, 2021, 150: 111467.

[14] ALQAISIA Z, MAHMOUD Y. Comprehensive study of partially shaded PV modules with overlapping diodes[J]. IEEE access, 2019, 7: 172665-172675.

[15] ABOUADANE H, FAKKAR A, SERA D, et al. Multiple-power-sample based P&O MPPT for fast-changing irradiance conditions for a simple implementation[J]. IEEE journal of photovoltaics, 2020, 10(5): 1481-1488.

[16] OWUSU-NYARKO I, ELGENEDY M A, ABDELSALAM I, et al. Modified variable step-size incremental conductance MPPT technique for photovoltaic systems[J]. Electronics, 2021, 10(19): 2331.

[17] SHEHU M M, DONG M, HU J S. Optimization of particle swarm based MPPT under partial shading conditions in photovoltaic systems[C]//16th IEEE Conference on Industrial Electronics and Applications (ICIEA), August 1-4, 2021, Chengdu, China. New York: IEEE, 2021: 267-272.

[18] WU Z, YU D. Application of improved bat algorithm for solar PV maximum power point tracking under partially shaded condition[J]. Applied soft computing, 2018, 62: 101-109.

[19] REZK H, FATHY A, ALY M. A robust photovoltaic array reconfiguration strategy based on coyote optimization algorithm for enhancing the extracted power under partial shadow condition[J]. Energy reports, 2021, 7: 109-124.

[20] ELTAMALY A M. An improved cuckoo search algorithm for maximum power point tracking of photovoltaic systems under partial shading conditions[J]. Energies, 2021, 14(4): 953.

[21] IBRAHIM M N, REZK H, AL-DHAIFALLAH M, et al. Solar array fed synchronous reluctance motor driven water pump: an improved performance under partial shading conditions[J]. IEEE access, 2016, 7: 77100-77115.

[22] RAMYAR A, IMAN-EINI H, FARHANGI S. Global maximum power point tracking method for photovoltaic arrays under partial shading conditions[J]. IEEE transactions on industrial electronics, 2017, 64(4): 2855-2864.

[23] TEUSCHL Y, TABORSKY B, TABORSKY M. How do cuckoos find their hosts? The role of habitat imprinting[J]. Animal behaviour, 1998, 56(6): 1425-1433.

[24] REYNLDS A M, FRYE M A. Free-flight odor tracking in drosophila is consistent with an optimal intermittent scale-free search[J]. Plos one, 2007, 2(4).

[25] AHMED J, SALAM Z. A maximum power point tracking (MPPT) for PV system using cuckoo search with partial shading capability[J]. Applied energy, 2014, 119(15): 118-130.

[26] YANG X S, DEB S. Cuckoo search: state-of-the-art and opportunities[C]//4th IEEE International Conference on Soft Computing & Machine Intelligence (ISCMI), November 23-24, 2017, Mauritius. New York: IEEE, 2017: 55-59.